Combined Effect of Specific Nucleation and Rubber Dispersion on Morphology and Mechanical Behavior of Isotactic Polypropylene

Jiří Kotek, Jaroslav Ščudla, Miroslav Šlouf, Miroslav Raab

Institute of Macromolecular Chemistry, Academy of Sciences of the Czech Republic, 162 06 Prague, Czech Republic

Received 30 January 2005; accepted 10 March 2006
DOI 10.1002/app.24426
Published online in Wiley InterScience (www.interscience.wiley.com).

ABSTRACT: This study aims to explore the joint effects of specific β-nucleation and rubber dispersion on morphology and mechanical behavior of materials derived from isotactic polypropylene. A β-nucleator (*N*,*N*′-dicyclohexylnaphthalene-2,6-dicarboxamide) and an amorphous EPM rubber were used for the modification of isotactic polypropylene. Four samples were investigated: neat polypropylene, the same polymer modified with 0.03 wt % of β-nucleator or with 15 wt % of dispersed rubber particles, and finally polypropylene containing both the β-nucleator and the rubber particles. Tensile and impact behavior were followed at room and cryogenic temperatures. It has been observed that the β-nucleation and rubber modification have brought about a similar macroscopic softening effect on the tensile mechanical behavior. Microscopy of fracture surfaces, however, has shown different toughening mechanisms caused by specific nucleation on one hand and by rubber dispersion on the other. While a distinct synergy effect of nucleation and rubber modification on the resulting toughness was found at low temperature, no such cooperative effect manifested itself at room temperature. © 2006 Wiley Periodicals, Inc. J Appl Polym Sci 103: 3539–3546, 2007

Key words: isotactic polypropylene; β-phase; toughness

INTRODUCTION

Isotactic polypropylene has been enjoying the fastest growth in consumption since its discovery. The reason is not only its favorable price/performance ratio, but also the possibility of tailoring its properties. The only disadvantage of this material is low toughness, especially at low temperatures. Several ways have been explored to improve the low temperature toughness, such as optimization of crystalline morphology and incorporation of a discrete rubbery phase (via blending or copolymerization). The rubber modification is traditionally one of the most widespread methods to improve impact properties of polypropylene. The relationship between morphology and toughness of rubber-modified polypropylene has been extensively studied (see, Ref. 1 and references therein). More recently, the effect of specific β-nucleation on toughness of polypropylene has been explored.[2–10] In the case of the nucleator based on *N*,*N*′-dicyclohexylnaphthalene-2,6-dicarboxamide, a nonmonotonic dependence between the nucleator content and toughness has been found.[10] The critical concentration of the nucleating agent giving maximum toughness and strain at break was found to be 0.03 wt %. At this concentration the long period (i.e., the distance between crystallites) has also shown a maximum. This correlation seems to support the notion that it is not the crystalline β-phase itself but rather a specific structure of the amorphous phase (induced by the β-crystallites) that imparts the enhanced toughness to the β-nucleated polypropylene. The ''magic'' nucleator concentration 0.03 wt %[10] was chosen in the experimental part of this study.

While the toughening mechanism caused by the rubber dispersion is generally understood, the structural processes behind the effects of the β-phase are still the subject of some controversy.[9,10] Nevertheless, it is clear that these two mechanisms principally differ. To our knowledge, only preliminary results on the possible synergy between the joint effect of β-nucleation and rubber modification have been available so far.[11] A comprehensive assessment of the joint effects of specific β-nucleation and rubber dispersion on the tensile and impact behavior of isotactic polypropylene is the object of the present study.

EXPERIMENTAL

Materials and specimen preparation

The starting material used throughout this study was a commercial-grade Ziegler-Natta isotactic polypropylene

Correspondence to: J. Kotek (kotek@imc.cas.cz).

Contract grant sponsor: Czech Science Foundation GA îCR; contract grant number: 106/02/P027.
Contract grant sponsor: Saxonian Government; contract grant number: project SMWK-Az. 4-7531.50-04-821-00/7.

Journal of Applied Polymer Science, Vol. 103, 3539–3546 (2007)

homopolymer Mosten 58.412 (Chemopetrol, Litvínov, Czech Republic). The material is characterized by a melt flow index of 3 g/10 min (230°C, 21.2*N*) and a weight-average molecular weight M_w of ~ 320,000.

A portion of the material was-modified with a selective β-nucleator NJ-Star NU-100 (Rika, Manchester, UK), based on *N*,*N*′-dicyclohexylnaphthalene-2,6-dicarboxamide in a concentration of 0.03 wt % using a master batch. The master batch was prepared by compounding polypropylene with 5 wt % of the nucleating agent in an internal mixer Brabender Plasticorder at 190°C and 60 rpm for 10 min. The β-nucleated polypropylene (labeled as PPβ) was prepared by subsequent compounding the master batch with PP pellets in a double-screw corotating extruder Berstorff ZE-25 ($L/D = 48$) at 150 rpm. The temperatures of heating zones were 220, 230, 240, 240, 240, 240, 230, 230, 220, and 220°C.

Ethylene–propylene copolymer Vistalon 404 (EPM) produced by Exxon Chemicals was used as rubber modifier. Infrared spectroscopy showed that it is a statistical copolymer and X-ray analysis confirmed its fully amorphous structure. Glass transition temperature of −53°C was determined by dynamic mechanical analysis.

Both the non-nucleated (PP) and β-nucleated (PPβ) polypropylenes pellets were blended with the EPM rubber in the above described extruder. Standard dumbbell specimens (DIN 53 455) were prepared by injection molding in the injection-molding machine Battenfeld BA 500 CD Plus. The processing conditions were described elsewhere.[12] The codes and compositions of the samples are listed in Table I.

Wide-angle X-ray scattering

A diffractometer P4 (Bruker, Karlsruhe, Germany) using Cu Kα radiation (monochromatized with primary graphite crystal) was used for the WAXS analysis of all studied materials. The diffractometer, equipped with area detection system HiStar/GADDS, which measured within radial scattering range $2\theta = 1.5$–40.5° was used in the transmission mode. The diameter of the detector pin hole was 0.5 mm (with a distance of 12 cm between the sample and detector) and the measurement time was 180 s. The total integral intensities I, and integral intensities diffracted by the crystalline part I_c were used for the determination of crystallinity, $X_c = I_c/I$. The experimental error has been evaluated from the difference between the real and approximated intensity profiles. The relative amount of the β-phase K_β in the crystalline portion of the material was calculated as:[6]

$$K_\beta = I^\beta_{300} \Big/ \left(I^\alpha_{110} + I^\alpha_{040} + I^\alpha_{130} + I^\beta_{300} \right),$$

where I^β_{300} is the integral intensity of 300 reflections of the β-phase and I^α_{110}, I^α_{040}, and I^α_{130} are the integral intensities of the 110, 040, and 130 reflections of the α-phase, respectively.

TABLE I
Sample Formulation

Code	Components	Composition (%)
PP	PP	100
PPβ	PP/β-nucleator	99.97/0.03
PP/EPM	PP/EPM rubber	85/15
PPβ/EPM	PPβ/EPM rubber	85/15

Differential scanning calorimetry

DSC thermograms were measured by a Perkin–Elmer DSC 7 (PerkinElmer, Boston, MA) in the temperature range of 10–210°C. Heating rate was 40 K min^{-1}. Representative samples containing both core and skin regions were cut out from the injection-molded specimens. The procedure for the assessment of crystallinity X_c and the β-phase content K_β has been described in our previous paper.[12]

Microscopy

Scanning electron microscope Vega (Tescan Brno, Czech Republic) was used for characterization of fracture surfaces and of material morphology. Cross sections of specimens perpendicular to the long axes were scratched with glass edge in liquid nitrogen to obtain flat surfaces without affecting the morphology. The surfaces were then etched in *n*-heptane for 3 min at room temperature. The morphology of the gold sputter coated specimens was studied. Secondary electron mode was used for imaging with 30 kV acceleration voltage.

An optical microscope Zetopan Pol (Reichert, Vienna, Austria) fitted with crossed polarizers was used for characterization of the spherulitic structure. Thin sections were prepared with a microtome and observed in transmitting polarized light.

Tensile measurements

A tensile tester Instron 5800 (Instron, High Wycombe, UK) equipped with a temperature cabinet was used for stress–strain measurements at room (23°C) and cryogenic (−40°C) temperatures. The specimens with a gauge length of 100 mm were deformed at a test speed of 20 mm min^{-1}. The tensile (Young's) modulus was determined using an extensometer (with a gauge length of 50 mm) at a test speed of 1 mm min^{-1}. For each material sample, five dumbbell specimens were tested under identical conditions.

Notched impact testing

Bar specimens 80 × 10 × 4 mm^3 were cut from central parts of injection-molded dumbbell specimens. The specimens were then notched on their narrow sides with a razor blade to the depth 2 mm. Specimens were tested at a speed of 1.5 ms^{-1} on a instrumented impact tester (PSW 4) with 4 J work capacity with a support span of 40 mm. The force (F)–deflection (f) curves were recorded. The total fracture energy A was split to initiation A_G and propagation (residual) A_R fracture energies as energy portions measured up to the maximum load F_{max} and from this point to full break, respectively.[13] The initiation energy was further divided into elastic A_{el} and plastic A_{pl} parts. The tests were carried out both at room and at cryogenic (−40°C) temperatures. In the case of low-temperature testing, the specimens were conditioned for 20 min in liquid nitrogen/ethanol bath. Temperature was controlled by the nitrogen/ethanol ratio and measured with an immersed thermometer. After conditioning, the specimens were quickly removed from the bath, immediately inserted to the support span and broken. At least 10 specimens of each sample at a given temperature were tested.

RESULTS AND DISCUSSION

Morphology

The overall crystallinity data, X_c, and the β-phase content, K_β, within the crystalline portion of the polypropylene as detected by WAXS and DSC are summarized in Table II. Figure 1 shows the corresponding WAXS radial reflections.

It is shown that neat polypropylene PP is composed entirely of the α-phase, while in β-modified polypropylene PPβ β-phase prevails. The total crystallinity X_c is approximately the same within experimental error. The aim of our morphological study was focused mainly on the function of rubber inclusions in both original and nucleated polypropylene matrices. The presence of the EPM rubber in both polypropylenes did not change the crystallinity X_c and β-phase content K_β significantly (PP/EPM, PPβ/EPM).

TABLE II
Comparison of WAXS and DSC Data for Starting Materials

	X_c (%)		K_β (%)	
Material	WAXS	DSC	WAXS	DSC
PP	58 ± 5	53	0	0
PPβ	57 ± 6	50	68 ± 6	62
PP/EPM	52 ± 6*	51*	0	0
PPβ/EPM	57 ± 6*	56*	64 ± 7*	59*

Standard deviations of the WAXS data reflect differences between the real diffractograms and the fitted curves.
* Data related to polypropylene matrix.

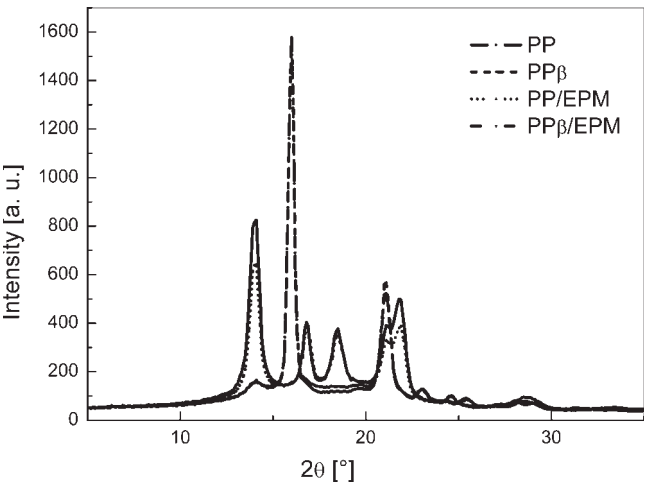

Figure 1 Integrated WAXS radial intensity distributions of the polypropylene-derived materials.

The morphology of both the rubber-modified systems is illustrated in Figure 2, where dark spots represent rubber particles etched with *n*-heptane. The mean diameter of rubber particles is approximately in the same range (∼ 0.5–2 μm) due to the same processing conditions and the rubber content (15%).

The presence of the nucleator in a very low concentration obviously does not change the rheology of the melt. Consequently, no significant differences in the size, shape and distribution of rubber particles between the rubber-modified systems (PP/EPM, PPβ/EPM) were observed. The morphology of the material modified both by β-nucleator and rubber particles has been characterized by light microscopy (Fig. 3). The spherulite diameter ranges approximately from 5 up to 15 μm; consequently, the rubber particles should be embedded within the spherulites. Indeed, the black spots in Figure 3 representing rubber inclusions could be found both at the interface and inside the spherulites.

Tensile behavior

Figure 4 shows typical stress–strain traces measured at both room temperature and low temperature for four polypropylene-derived samples. The experimental temperatures (23°C, −40°C) were selected intentionally well above the glass transition temperature T_g of amorphous polypropylene (−10°C) in one case and below the T_g of polypropylene but above the T_g of the rubber modifier (−53°C) in the other. From the experimental stress–strain curves the characteristic mechanical parameters were derived: Young modulus E, yield stress σ_y and strain at break ε_b. The average values of these characteristics are summarized

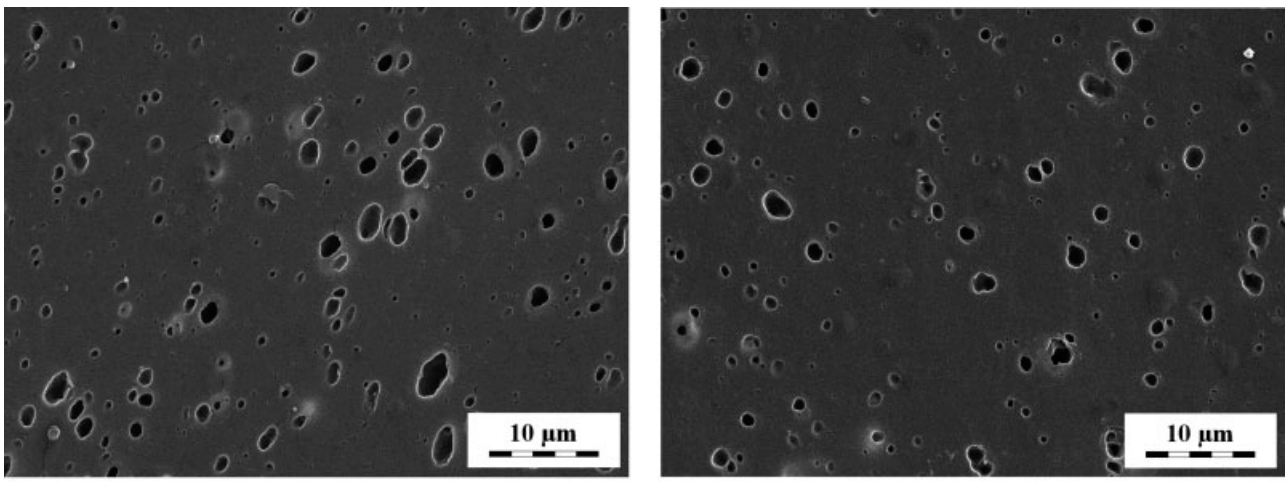

Figure 2 Morphology of rubber-toughened polypropylene with two different matrices (a) α-crystalline matrix (PP/EPM), (b) β-crystalline matrix (PPβ/EPM).

in Table III. Neat isotactic polypropylene (PP) has shown the highest yield stress σ_y at both experimental temperatures, the σ_y values decreasing in the order PP > PPβ > PP/EPM > PPβ/EPM. The values of the *E* modulus and the local (natural) draw ratio determined from the displacement of ink marks decreased in the same order. The softening effect of the β-modification and its structural explanation has already been discussed in our previous publications.[5,10] At room temperature the ε_b value could not be determined as the drawability of all samples exceeded the crosshead travel range of the tensile tester; at the given gauge length the maximum travel range corresponded to strain at break of 650%. At the cryogenic temperature the drawability was suppressed substantially. Moreover, a dramatic increase in the yield stress, σ_y, and particularly in the Young modulus, *E*, are manifested. Nevertheless, all samples showed distinct yielding even under cryogenic conditions, in particular, the PPβ/EPM sample retained a marked softening effect introduced by the joint effect of specific nucleation and rubber dispersion.

Visual inspection has revealed that at room temperature the specimens deformed in a manner typical of semicrystalline polymers with localized yielding (necking), stress whitening, and an extended region of cold drawing and strain strengthening. It is well known that in the neck shoulder a transition between a spherulitic (or lamellar) structure into a fibrillar morphology takes place. With the samples modified by specific nucleation and/or rubber dispersion, the neck became more diffuse and the stress whitening less pronounced, but nonuniform deformation persisted. As already shown for the β-nucleated samples,[14] with increasing local elongation λ the content of crystalline β-phase decreases as a result of the β → α solid-state transformation in the neck shoulder.

Unlike the modified samples, which develop diffuse and smoothly propagating neck shoulders, the neat polypropylene shows a sharp neck shoulder. Its propagation along the specimen during drawing is not quite smooth, but rather stepwise, as was also recorded in the oscillating stress–strain curve (Fig. 4). These stress oscillations could be ascribed to temperature fluctuation in the narrow ''processing'' zone.[15]

The softening of polypropylene matrix by specific β-modification also influenced the local deformation of the embedded rubber particles. As shown in Figure 5, their extension along the draw direction is

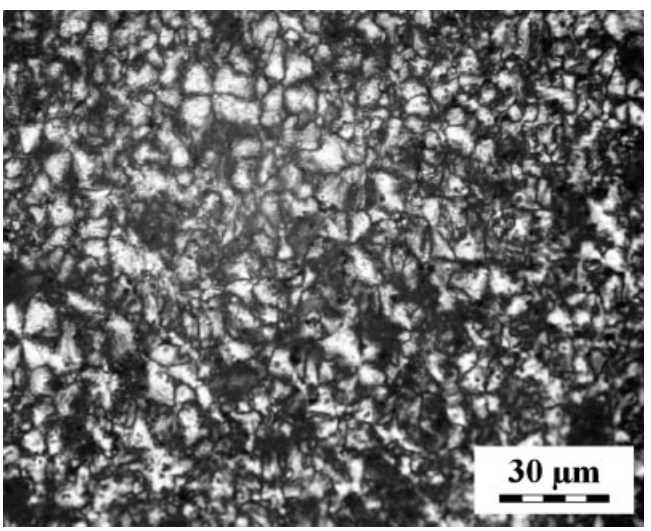

Figure 3 Birefrigence micrograph of core regions of polypropylene modified by both β-nucleator and EPM rubber (PPβ/EPM).

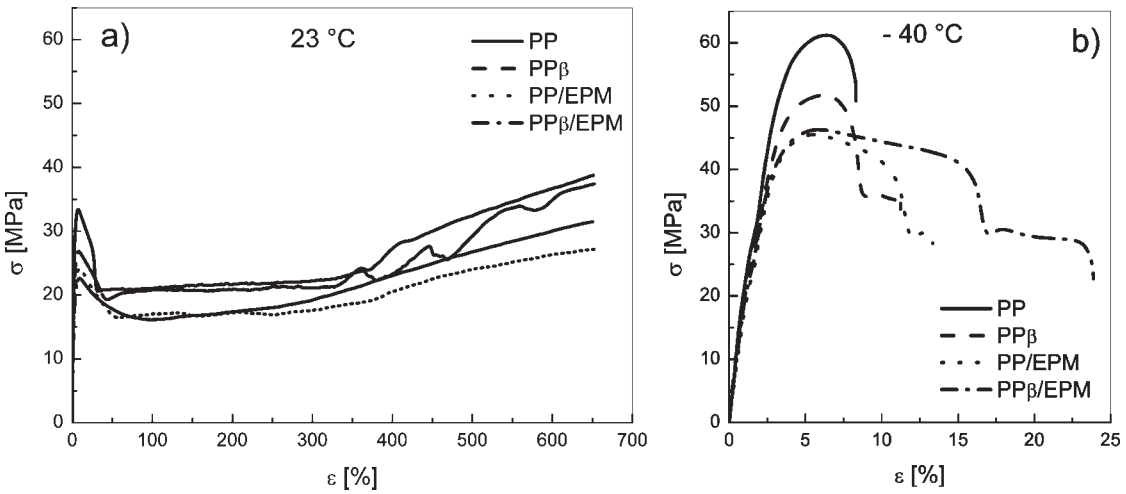

Figure 4 Stress–strain curves of four polypropylene-derived materials at two different temperatures, (a) 23°C, (b) −40°C.

less pronounced as compared with the neat polypropylene matrix. At the same time, strain fibrillation is suppressed in the nucleated matrix.

Impact behavior

Typical load-deflection curves of all materials obtained from instrumented impact tests are depicted in Figure 6. The corresponding parts of total fracture energy are presented in Figure 7. At room temperature (Fig. 6a) neat polypropylene exhibits brittle fracture with an almost linear load–deflection curve. The plastic part A_{pl} of the crack initiation energy is negligible, as it corresponds to depressed plastic deformation at the notch tip. The β-nucleation brought about a dramatic increase in total fracture energy. The load–deflection curve shows that the onset of the crack propagation occurs at substantially higher level of both force and deflection. Moreover, a certain amount of crack propagation energy also contributes to higher material toughness. The dispersion of rubber particles at the concentration 15 wt % does not lead to such a toughening effect as β-nucleation. Detailed analysis shows that this difference is caused mainly by low stress level at crack initiation. The maximum force of PP/EPM sample is comparable with that of neat PP. The additional modification of the β-nucleated polypropylene with EPM rubber does not bring about any substantial changes in fracture energy (Fig. 7). Both initial and propagation energies of these two materials are comparable. Nevertheless, the shapes of the load–deflection curves are different. The crack in rubber-modified material PPβ/EPM starts to propagate at lower force, but at higher deflection. A comparison of the fracture surfaces of rubber-modified materials with two different matrices (Fig. 8) shows a different fracture micromechanism. While the fracture surface of the blend with nonmodified matrix (Fig. 8a) is relatively smooth, that of the material with β-nucleated matrix is rough, indicating many sites of local plasticity. It is clear that orientation of the β-modified polypropylene in these regions absorbs more energy during impact. At the same time, the oriented polymer forms obstacles to the crack propagating perpendicularly to the orientation direction. This is referred to as the Cook–Gordon mechanism.[16]

At −40°C all materials break in a brittle manner, as indicated by the force–deflection diagrams (Fig. 6b). With all materials, only the elastic part of crack initiation energy contributes to total fracture energy. All the force–deflection diagrams are linear, ending in a sharp drop after reaching the maximum. Nevertheless, the modification brought about an increase in both deflection and force at the onset of crack initiation. Similarly as of the room temperature, the material modified solely by rubber (PP/EPM) shows

TABLE III
Tensile Mechanical Characteristics of Polypropylene-Derived Materials

	23°C			−40°C		
Sample	E (MPa)	σ_y (MPa)	ε_b (%)	E (MPa)	σ_y (MPa)	ε_b (%)
PP	1560 ± 100	33.1 ± 0.3	>650	6000 ± 300	61.1 ± 1.0	8.4 ± 0.3
PPβ	1400 ± 40	28.4 ± 0.1	>650	5300 ± 200	52.7 ± 1.0	11.2 ± 2.6
PP/EPM	1000 ± 20	24.2 ± 0.2	>650	4400 ± 60	45.0 ± 0.4	14.4 ± 3.4
PPβ/EPM	1050 ± 50	23.7 ± 0.3	>650	3800 ± 150	46.2 ± 0.2	18.6 ± 5.3

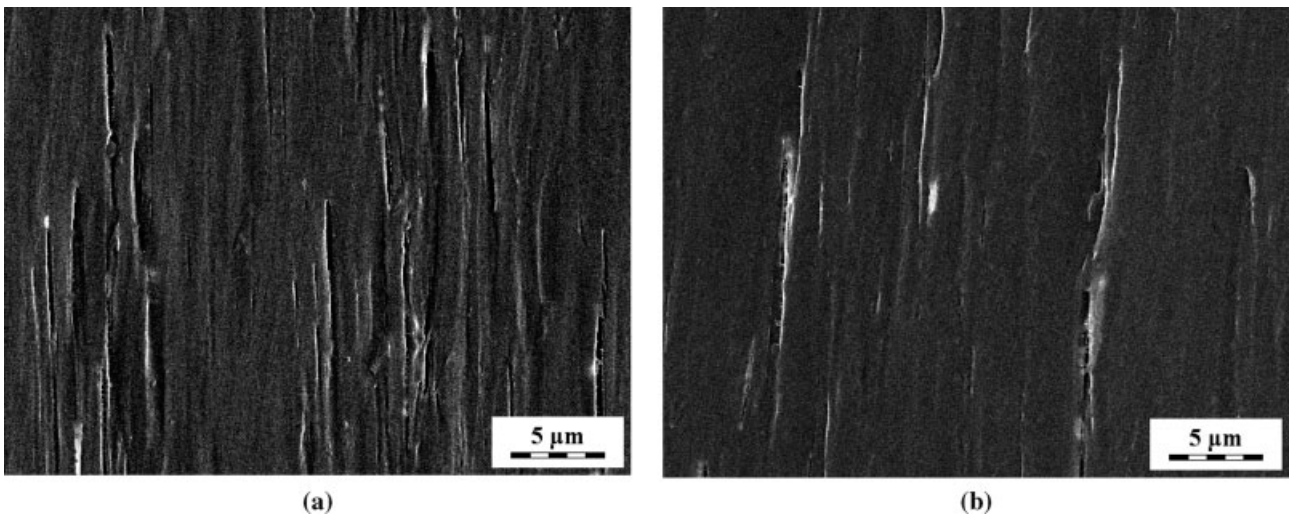

Figure 5 Morphology of drawn rubber-modified polypropylenes: (a) PP/EPM ($\lambda = 7$) (b) PPβ/EPM ($\lambda = 6.6$).

the smallest increase in fracture energy (Fig. 7). Again, the β-nucleation has proven to be more effective in toughening than the applied rubber modification. Interestingly enough, the combination of both rubber and β-modification developed a significant synergy effect on toughness, which has not been manifested at room temperature. Local deformation micromechanisms are visible at fracture surfaces (Fig. 8).

Structural model

The two polypropylene modifiers used in this study show similar effects on macroscopic mechanical behavior. They both cause softening of the material as expressed by a decrease in the modulus of elasticity and yield stress. The decrease in the yield stress is particularly pronounced for the rubber modification (sample PP/EPM). The different modifiers, however, basically differ in their toughening micromechanisms. It is generally accepted that the toughening effect of rubber inclusions is caused by multiple shear banding in their close vicinity. On the other hand, the effect of the β-modification is very likely associated with a specific structure of the amorphous phase induced by the presence of β-crystallites.[5] Indeed, toughness is a matrix-controlled property, both in composites and semicrystalline polymers.

When the both modifiers coexist, the distinguishing of their effects is difficult. Nevertheless, the difference between the toughening effect of dispersed rubber and β-modification can be seen in the effect of orientation. While the rubber particles dissipate mechanical energy in larger volume, the β-modification additionally imparts the ability of orientation. The former mechanism of energy dissipation occurs of the expense of lowering the stress at crack initiation. At the low temperature, the rubber approaches

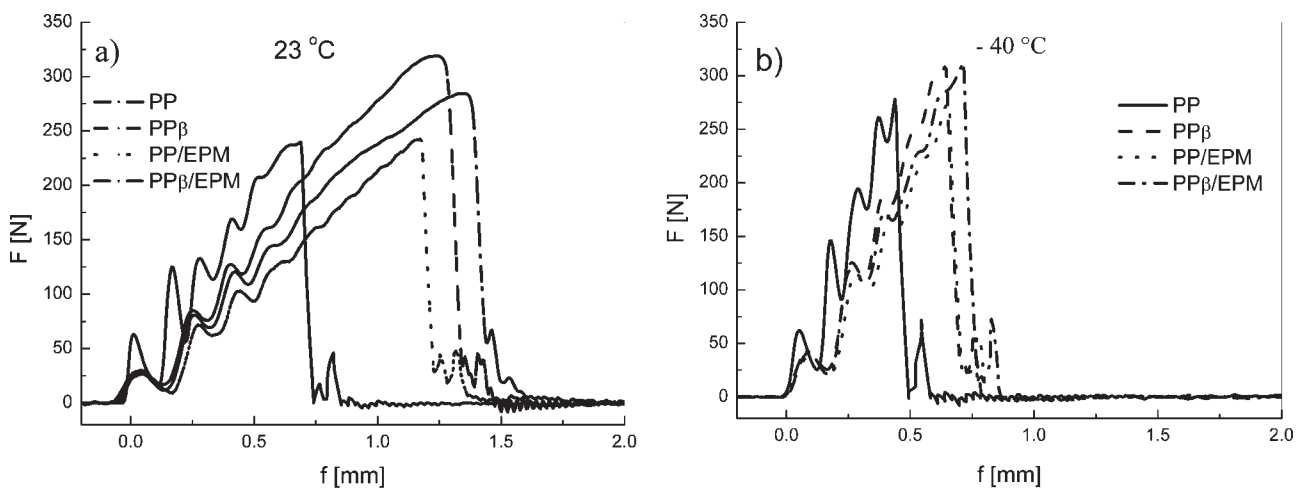

Figure 6 Typical impact load–deflection curves at (a) 23°C and (b) −40°C.

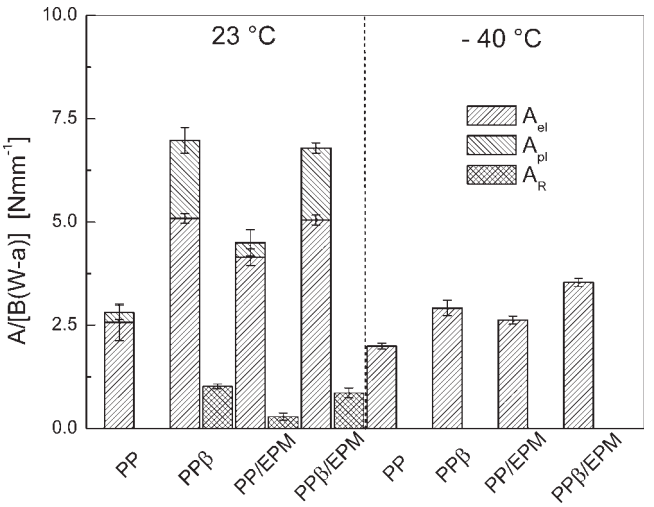

Figure 7 Deformation energy values A for polypropylene-derived materials. Total fracture energy A is split into the initiation energy A_G ($A_{el} + A_{pl}$) and the propagation energy A_R.

its glass transition temperature and, consequently, the stiffness decreases only little and the stress at crack initiation approaches a higher level, while the particles still act as stress concentrators inducing energy dissipation. When the β-phase additionally increases the orientation at the crack tip, a synergy of both modifiers appears.

CONCLUSIONS

Based on the structural, thermal, mechanical, and fracture analyses of the modified polypropylenes presented above, the following conclusions can be drawn:

1. The addition of 0.03 wt % of a specific β-nucleator induced predominant formation of the crystalline β-phase. On the other hand, the dispersion

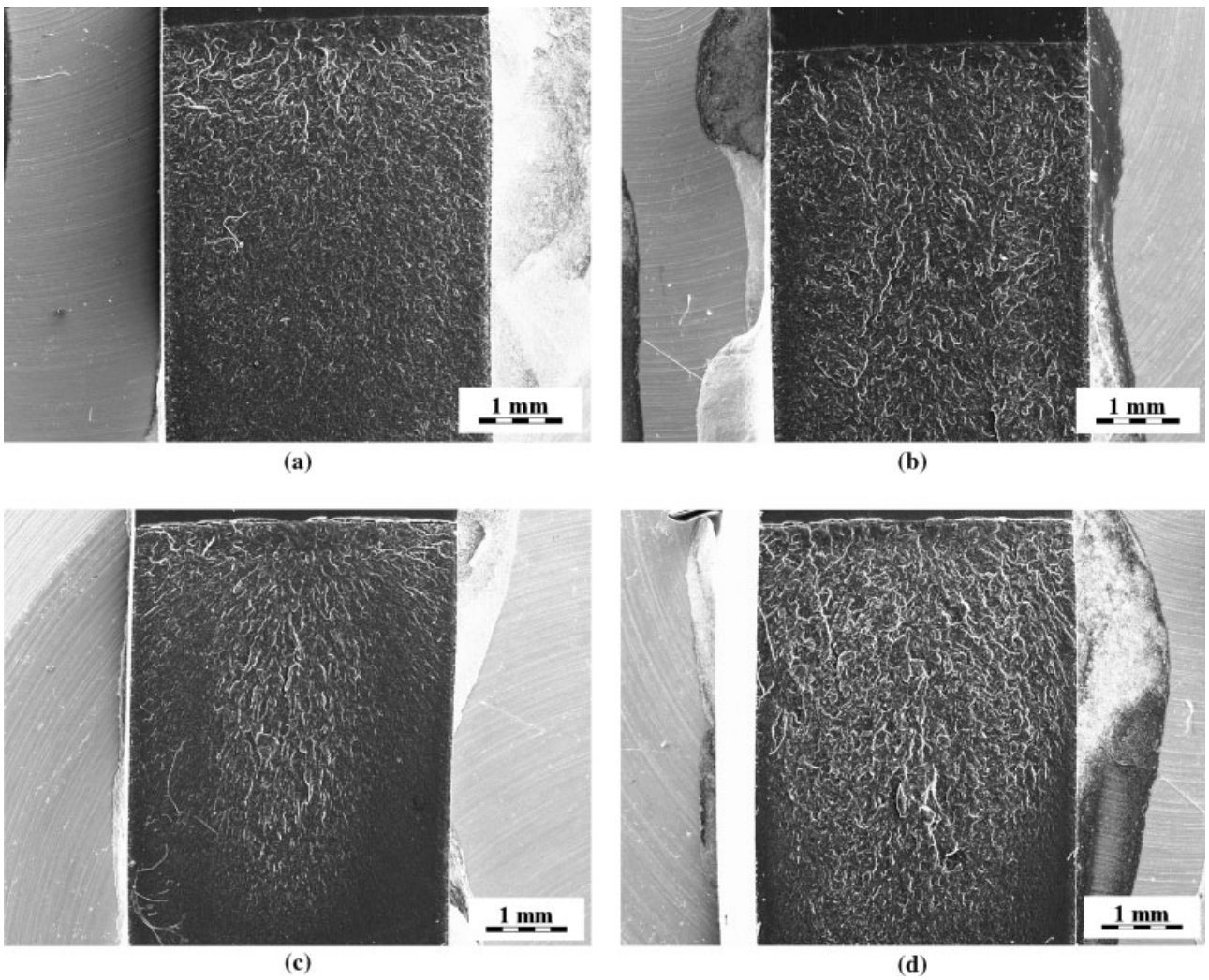

Figure 8 Scanning electron micrographs of fracture surfaces of rubber-modified polypropylenes measured at two different temperatures: (a) PP/EPM, $T = 23°C$, (b) PPβ/EPM, $T = 23°C$, (c) PP/EPM, $T = -40°C$, (d) PPβ/EPM, $T = -40°C$.

of the EPM rubber had virtually no effect on the β-phase content in the polypropylene matrix.
2. Typical rubber particles with a diameter of 0.5–2 μm are distinctly smaller than the polypropylene spherulites that are larger by one order of magnitude. Consequently, the particles are located both inside the spherulites and of the spherulite boundary.
3. Both the β-nucleation and rubber modification at given concentrations have brought about a similar softening effect on the tensile mechanical behavior. At the same time, each of them increased the toughness. The deflection at the onset of crack propagation at room temperature increased in the order PP < PP/EPM < PPβ < PPβ/EPM. The β-nucleation led to higher toughness than the sole rubber modification. At room temperature no synergy was observed when both the modifiers were applied simultaneously.
4. At −40°C the β-nucleated sample has shown higher toughness than did the rubber-modified polypropylene. On the other hand, a synergy effect occurred in PPβ/EPM-modified material showing the highest toughness. This effect was ascribed to higher stiffness of the rubber inclusions at the cryogenic temperature and additional orientation of the β-modification. The evaluation of experimental scatter has shown that the observed trends in mechanical characteristic are statistically significant.

References

1. Karger-Kocsis, J., Ed. Polypropylene: An A-Z Reference; Kluwer: Dordrecht, 1999.
2. Varga, J. J Macromol Sci B 2002, 41, 1121.
3. KargerKocsis, J.; Varga, J.; Ehrenstein, G. W. J Appl Polym Sci 1997, 64, 2057.
4. Fujiyama, M. Int Polym Proc 1998, 13, 411.
5. Raab, M.; Kotek, J.; Baldrian, J.; Grellmann, W. J Appl Polym Sci 1998, 69, 2255.
6. Tordjeman, P.; Robert, C.; Marin, G.; Gerard, P. Eur Phys J 2001, 4, 459.
7. Tjong, S. C.; Shen, J. S.; Li, R. K. Y. Polym Eng Sci 1996, 36, 100.
8. Labour, T.; Vigier, G.; Seguela, R.; Gauthier, C.; Orange, G.; Bomal, Y. J Polym Sci Part B: Polym Phys 2001, 40, 31.
9. Chen, H. B.; Karger-Kocsis, J.; Wu, J. S.; Varga, J. Polymer 2002, 43, 650514.
10. Kotek, J.; Raab, M.; Baldrian, J.; Grellmann, W. J Appl Polym Sci 2002, 85, 1174.
11. Grein, C.; Plummer, C. J. G.; Kausch, H.-H.; Germain, Y.; Beguelin, P. Polymer 2002, 43, 3279.
12. Scudla, J.; Eichhorn, K. J.; Raab, M.; Schmidt, P.; Jehnichen, D.; Häußler, L. Macromol Symp 2002, 184, 371.
13. Grellmann, W.; Lach, R.; Seidler, S. Int J Fracture 2002, 114, L9.
14. Scudla, J.; Raab, M.; Eichhorn, K. J.; Strachota, A. Polymer 2003, 44, 4655.
15. Raab, M.; Hnat, V. Int J Fracture 1984, 24, R93.
16. Raab, M.; Schultz, E.; Sova, M. Polym Eng Sci 1993, 33, 1438.